Adaptive Robust Precision Motion Control of Linear Motors With Negligible Electrical Dynamics: Theory and Experiments

Li Xu and Bin Yao, *Member, IEEE*

***Abstract*—Linear motors offer several advantages over their rotary counterparts in many applications requiring linear motion by eliminating mechanical transmission mechanisms. However, these advantages are obtained at the expense of added difficulties in controlling such a system. This paper studies the high performance robust motion control of an epoxy core linear motor, which has negligible electrical dynamics due to the fast response of the electrical subsystem. A discontinuous projection based adaptive robust controller (ARC) is first constructed. The controller theoretically guarantees a prescribed transient performance and final tracking accuracy in general, while achieving asymptotic tracking in the presence of parametric uncertainties. A desired compensation ARC scheme is then presented, in which the regressor is calculated using reference trajectory information only. The resulting controller has several implementation advantages such as less on-line computation time, reduced effect of measurement noise, a separation of robust control design from parameter adaptation, and a faster adaptation rate. Both schemes are implemented and compared on an epoxy core linear motor. Extensive comparative experimental results are presented to illustrate the effectiveness and the achievable control performance of the two ARC designs.**

***Index Terms*—Adaptive control, linear motors, motion control, precision manufacturing, robust control.**

I. Introduction

MODERN mechanical systems, such as semiconductor manufacturing equipment, often require high-speed/high-accuracy linear motions. These linear motions are usually realized using rotary motors with mechanical transmission mechanisms such as reduction gears and lead screw. Such mechanical transmissions not only significantly reduce linear motion speed and dynamic response, but also introduce backlash, large frictional and inertial loads, and structural flexibility. As an alternative, direct drive linear motors, which eliminate the use of mechanical transmissions, show promise for widespread use in high-speed/high-accuracy positioning systems [1]–[3].

Significant effort has been devoted to solving the difficulties in controlling linear motors [1], [2], [4], [5], [3], [6]. Early work includes the H_∞-based linear robust control methods proposed by Alter and Tsao in [1], [2], the disturbance observer (DOB) [7], [5] based disturbance compensation method in [4], and feedforward nonlinear ripple force compensation in [3]. Practically, H_∞ design [1], [2] may be conservative for high-speed/high-accuracy tracking control. The DOB design [7], [5], [4] may not handle discontinuous disturbances such as Coulomb friction well and cannot deal with large extent of parametric uncertainties, as shown both theoretically and experimentally by Yao, *et al.* in [8]. The feedforward compensation based on off-line identification model [3] may be too sensitive and costly to be useful. In [6], a neural-network-based learning feedforward controller was proposed. However, overall closed-loop stability is not guaranteed, and instability may occur at high-speed movements [6].

In [9], the idea of adaptive robust control (ARC) [10]–[12] was generalized to provide a rigorous theoretic framework for the high performance motion control of an iron core linear motor. The controller takes into account the effect of model uncertainties coming from the inertia load, friction, force ripple and electrical parameters, etc. In particular, based on the structure of the motor model, on-line parameter adaptation is utilized to reduce the effect of parametric uncertainties while the uncompensated uncertain nonlinearities are handled effectively via certain robust control laws for high performance. As a result, time-consuming and costly rigorous off-line identification of friction and ripple forces is avoided without sacrificing tracking performance.

In this paper, the ARC algorithm proposed in [9] is first applied on an epoxy core linear motor in which the current dynamics is neglected due to the fast electric response. However, as pointed out in [13], this algorithm may have several potential implementation problems since the regressor depends on the states of the system. As a remedy, a desired compensation ARC [14], [13] in which the regressor is calculated by reference trajectory information only is developed. The proposed new ARC controller has several implementation advantages such as reducing on-line computation time, separating the robust control design from parameter adaptation process, reducing the effect of measurement noise, and having a faster adaptation process. Finally, both ARC schemes are implemented and compared on an epoxy core linear motor. Comparative experimental results are presented to show the advantages and the drawbacks of each method.

Manuscript received February 2, 2000; revised August 3, 2001. Recommended by Technical Editor K. Ohnishi. This work was supported in part by the National Science Foundation under the CAREER Grant CMS-9734345 and in part by the Purdue Research Foundation. This work was presented in part at the 2000 American Control Conference, Chicago IL, June 2000.

The authors are with the School of Mechanical Engineering, Purdue University, West Lafayette, IN 47907 USA (e-mail: byao@ecn.purdue.edu).

Publisher Item Identifier S 1083-4435(01)10732-5.

II. Problem Formulation and Dynamic Models

The linear motor considered here is a current-controlled three-phase epoxy core motor driving a linear positioning stage supported by recirculating bearings. To fulfill the high performance requirements, the model is obtained to include most nonlinear effects like friction and ripple forces. In the derivation of the model, the current dynamics is neglected in comparison to the mechanical dynamics due to the much faster electric response. The mathematical model of the system can be described by the following equations:[1]

$$\begin{aligned} M\ddot{y} &= u - F \\ F &= F_f + F_r - F_d \end{aligned} \tag{1}$$

where y represents the position of the inertia load, M is the mass of the inertia load plus the coil assembly, u is the input voltage to the motor, F is the normalized lumped effect of uncertain nonlinearities such as friction F_f, ripple forces F_r, and external disturbance F_d (e.g., cutting force in machining). While there have been many friction models proposed [15], a simple and often adequate approach is to regard friction force as a static nonlinear function of the velocity, i.e., $F_f(\dot{y})$, which is given by

$$F_f(\dot{y}) = B\dot{y} + F_{fn}(\dot{y}) \tag{2}$$

where B is an equivalent viscous friction coefficient of the system, F_{fn} is the nonlinear friction term which can be modeled as [15], [16]

$$F_{fn}(\dot{y}) = -\left[f_c + (f_s - f_c)e^{-|\dot{y}/\dot{y}_s|^{\xi}}\right]\operatorname{sgn}(\dot{x}) \tag{3}$$

where f_s is the level of static friction, f_c is the minimum level of Coulomb friction, and $\dot{y}_s$ and ξ are empirical parameters used to describe the Stribeck effect. In practice, due to the inaccuracy of the positioning stage and ball bearings, the friction force may also depend on position y. This phenomenon is still captured by (1), since the bounded variation of position-dependent friction can be lumped into the external disturbance F_d. Thus, considering (2), we can rewrite (1) as

$$\begin{aligned} \dot{x}_1 &= x_2 \\ M\dot{x}_2 &= u - Bx_2 - F_{fn} + \Delta \\ y &= x_1 \end{aligned} \tag{4}$$

where $x = [x_1, x_2]^T$ represents the state vector of the position and velocity, y is the position output, and $\Delta \triangleq (F_d - F_r)$ represents the lumped disturbance.

Let $y_r(t)$ be the reference motion trajectory. The objective is to synthesize a control input u such that the output y tracks $y_r(t)$ as closely as possible in spite of various model uncertainties.

III. Adaptive Robust Control of Linear Motors

A. Design Models and Assumptions

It is seen that the friction model (3) is discontinuous at $x_2 = 0$. Thus, one cannot use this model for friction compensation since there is no way that the motor can generate a discontinuous motor force to accomplish the task. To bypass this technical difficulty, a simple continuous friction model will be used to approximate the actual discontinuous friction model (3) for model compensation; the model used in the paper is given by $\overline{F}_{fn} = A_f S_f(x_2)$, where the amplitude A_f is unknown, and $S_f(x_2)$ is a continuous function. The second equation of (4) can, thus, be written as

$$M\dot{x}_2 = u - Bx_2 - A_f S_f + d \tag{5}$$

where $d = \overline{F}_{fn} - F_{fn} + \Delta$.

In general, the system is subjected to parametric uncertainties due to the variations of M, B, and A_f, and the nominal value of the lumped disturbance d, d_n. In order to use parameter adaptation to reduce parametric uncertainties for an improved performance, it is necessary to linearly parameterize the state space-equation in terms of a set of unknown parameters. To achieve this, define the unknown parameter set $\theta = [\theta_1, \theta_2, \theta_3, \theta_4]$ as $\theta_1 = M, \theta_2 = B, \theta_3 = A_f$, and $\theta_4 = d_n$. The state space-equation can thus be linearly parameterized in terms of θ as

$$\dot{x}_1 = x_2 \tag{6}$$

$$\theta_1\dot{x}_2 = u - \theta_2 x_2 - \theta_3 S_f + \theta_4 + \tilde{d} \tag{7}$$

where $\tilde{d} = d - d_n$. The following practical assumption is made.

Assumption 1: The extent of the parametric uncertainties and uncertain nonlinearities are known, i.e.

$$\theta \in \Omega_\theta \triangleq \{\theta: \theta_{\min} < \theta < \theta_{\max}\} \tag{8}$$

$$\tilde{d} \in \Omega_d \triangleq \{\tilde{d}: |\tilde{d}| \le \delta_d\} \tag{9}$$

where $\theta_{\min} = [\theta_{1\min}, \ldots, \theta_{4\min}]^T$, $\theta_{\max} = [\theta_{1\max}, \ldots, \theta_{4\max}]^T$, and δ_d are known. In (8), the operation $<$ for two vectors is performed in terms of the corresponding elements of the vectors. ◇

B. Notations and Discontinuous Projection

Let $\hat{\theta}$ denote the estimate of θ and $\tilde{\theta}$ the estimation error (i.e., $\tilde{\theta} = \hat{\theta} - \theta$). In view of (8), the following adaptation law with discontinuous projection modification can be used

$$\dot{\hat{\theta}} = Proj_{\hat{\theta}}(\Gamma\tau) \tag{10}$$

where $\Gamma > 0$ is a diagonal matrix, τ is an adaptation function to be synthesized later. The projection mapping $Proj_{\hat{\theta}}(\bullet) = [Proj_{\hat{\theta}_1}(\bullet_1), \ldots, Proj_{\hat{\theta}_p}(\bullet_p)]^T$ is defined in [17], [18] as

$$Proj_{\hat{\theta}_i}(\bullet_i) = \begin{cases} 0, & \text{if } \hat{\theta}_i = \theta_{i\max} \text{ and } \bullet_i > 0 \\ 0, & \text{if } \hat{\theta}_i = \theta_{i\min} \text{ and } \bullet_i < 0 \\ \bullet_i, & \text{otherwise.} \end{cases} \tag{11}$$

It can be shown [10] that for any adaptation function τ, the projection mapping used in (11) guarantees

$$\begin{aligned} &\mathbf{P1} \quad \hat{\theta} \in \Omega_\theta \triangleq \{\hat{\theta}: \theta_{\min} \le \hat{\theta} \le \theta_{\max}\} \\ &\mathbf{P2} \quad \tilde{\theta}^T(\Gamma^{-1}Proj_{\hat{\theta}}(\Gamma\tau) - \tau) \le 0 \quad \forall\tau. \end{aligned} \tag{12}$$

C. ARC Controller Design

Define a switching-function-like quantity as

$$p = \dot{e} + k_1 e = x_2 - x_{2eq} \qquad x_{2eq} \triangleq \dot{y}_d - k_1 e \tag{13}$$

[1]Note that all terms are written in terms of the unit of input voltage.

where $e = y - y_d(t)$ is the output tracking error, $y_d(t)$ is the desired trajectory to be tracked by y, and k_1 is any positive feedback gain. If p is small or converges to zero exponentially, then the output tracking error e will be small or converge to zero exponentially since $G_p(s) = e(s)/p(s) = 1/(s + k_1)$ is a stable transfer function. So the rest of the design is to make p as small as possible. Differentiating (13) and noting (7), one obtains

$$\begin{aligned} M\dot{p} &= u - \theta_1 \dot{x}_{2eq} - \theta_2 x_2 - \theta_3 S_f + \theta_4 + \tilde{d} \\ &= u + \varphi^T \theta + \tilde{d} \end{aligned} \tag{14}$$

where $\dot{x}_{2eq} \triangleq \ddot{y}_d - k_1 \dot{e}$ and $\varphi^T = [-\dot{x}_{2eq}, -x_2, -S_f(x_2), 1]$. Noting the structure of (14), the following ARC control law is proposed:

$$u = u_a + u_s \qquad u_a = -\varphi^T \hat{\theta} \tag{15}$$

where u_a is the adjustable model compensation needed for achieving perfect tracking, and u_s is a robust control law to be synthesized later. Substituting (15) into (14), and then simplifying the resulting expression, one obtains

$$M\dot{p} = u_s - \varphi^T \tilde{\theta} + \tilde{d}. \tag{16}$$

The robust control function u_s consists of two terms given by

$$u_s = u_{s1} + u_{s2} \qquad u_{s1} = -k_2 p \tag{17}$$

where u_{s1} is used to stabilize the nominal system, and u_{s2} is a robust feedback term used to attenuate the effect of model uncertainties as follows. Noting Assumption 1 and P1 of (12), there exists a u_{s2} such that the following two conditions are satisfied:

$$\begin{aligned} &\text{i)} \quad p\{u_{s2} - \varphi^T \tilde{\theta} + \tilde{d}\} \le \varepsilon \\ &\text{ii)} \quad p u_{s2} \le 0 \end{aligned} \tag{18}$$

where ε is a design parameter which can be arbitrarily small. Essentially, i of (18) shows that u_{s2} is synthesized to dominate the model uncertainties coming from both parametric uncertainties $\tilde{\theta}$ and uncertain nonlinearities $\tilde{d}$, and ii of (18) is to make sure that u_{s2} is dissipating in nature so that it does not interfere with the functionality of the adaptive control part u_a.

Theorem 1: If the adaptation function in (10) is chosen as

$$\tau = \varphi p \tag{19}$$

then the ARC control law (15) guarantees the following.

A) In general, all signals are bounded. Furthermore, the positive definite function V_s defined by

$$V_s = \tfrac{1}{2} M p^2 \tag{20}$$

is bounded above by

$$V_s \le \exp(-\lambda t) V_s(0) + \frac{\varepsilon}{\lambda} [1 - \exp(-\lambda t)] \tag{21}$$

where $\lambda = 2k_2/\theta_{1\max}$.

B) If after a finite time t_0, there exist parametric uncertainties only (i.e., $\tilde{d} = 0, \forall t \ge t_0$), then, in addition to results in A), zero final tracking error is also achieved, i.e., $e \longrightarrow 0$ and $p \longrightarrow 0$ as $t \longrightarrow \infty$.

Proof: See Appendix I.

Remark 1: Let h be any smooth function satisfying

$$h \ge \|\theta_M\| \, \|\varphi\| + \delta_d \tag{22}$$

where $\theta_M = \theta_{\max} - \theta_{\min}$. Then, one smooth example of u_{s2} satisfying (18) is given by

$$u_{s2} = -\frac{1}{4\varepsilon} h^2 p. \tag{23}$$

Other smooth or continuous examples of u_{s2} can be worked out in the same way as in [10]–[12]. ♢

Remark 2: To further reduce transient tracking error, the idea of trajectory initialization [10], [19] can be utilized. Namely, instead of simply letting the desired trajectory for the controller be the actual reference trajectory or position [i.e., $y_d(t) = y_r(t)$], $y_d(t)$ can be generated using a filter. For example, $y_d(t)$ can be generated by the following third order stable system

$$y_d^{(3)} + \beta_1 y_d^{(2)} + \beta_2 y_d^{(1)} + \beta_3 y_d = y_r^{(3)} + \cdots + \beta_3 y_r \tag{24}$$

with the initial conditions given by $y_d(0) = x_1(0)$, $\dot{y}_d(0) = \dot{x}_1(0)$, and $\ddot{y}_d(0) = \ddot{x}_1(0)$. By doing so, $V_s(0) = 0$ and the transient tracking error is reduced as seen from (21). ♢

IV. Desired Compensation ARC (DCARC)

In the ARC design presented in Section III, the regressor φ in the model compensation u_a (15) and adaptation function τ (19) depends on state x. Such an adaptation structure may have several potential implementation problems [13]. First, φ has to be calculated on-line based on the actual measurement of the velocity x_2. Thus, the effect of measurement noise may be severe, and a slow adaptation rate may have to be used, which in turn reduces the effect of parameter adaptation. Second, despite that the intention of introducing u_a is for model compensation, because of φ, u_a depends on the actual feedback of the state also. Although theoretically the effect of this added implicit feedback loop has been considered in the robust control law design as seen from condition i) of (18), practically, there still exists certain interactions between the model compensation u_a and the robust control u_s. This may complicate the controller gain tuning process in implementation. In [20], Sadegh and Horowitz proposed a desired compensation adaptation law, in which the regressor is calculated by desired trajectory information only. The idea was then incorporated in the ARC design in [14], [13]. In the following, the desired compensation ARC is applied on the linear motor system, and particular structure of the linear motor dynamics is utilized to obtain less restrictive conditions on the selection of robust feedback gains.

The proposed desired compensation ARC law and the adaptation function have the same form as (15) and (19), respectively, but with regressor φ substituted by the desired regressor φ_d

$$u = u_a + u_s \qquad u_a = -\varphi_d^T \hat{\theta} \qquad \tau = \varphi_d p \tag{25}$$

where $\varphi_d^T = [-\ddot{y}_d, -\dot{y}_d, -S_f(\dot{y}_d), 1]$. Substituting (25) into (14), and noting $x_2 = \dot{y}_d + \dot{e}$, one obtains

$$M\dot{p} = u_s - \varphi_d^T \tilde{\theta} + \underbrace{(\theta_1 k_1 - \theta_2)\dot{e} + \theta_3 [S_f(\dot{y}_d) - S_f(x_2)]}_{} + \tilde{d} \tag{26}$$

Comparing (26) with (16), it can be seen that two additional terms (underbraced) appear, which may demand a strengthened

robust control function u_s for a robust performance. Applying mean value theorem, we have

$$S_f(x_2) - S_f(\dot{y}_d) = g(x_2, t)\dot{e} \tag{27}$$

where $g(x_2, t)$ is a nonlinear function. The strengthened robust control function u_s has the same form as (17)

$$u_s = u_{s1} + u_{s2} \qquad u_{s1} = -k_{s1}p \tag{28}$$

but with k_{s1} being a nonlinear gain large enough such that the matrix A defined below is positive-definite

$$A = \begin{bmatrix} k_{s1} - k_2 - \theta_1 k_1 + \theta_2 + \theta_3 g & -\frac{1}{2}k_1(\theta_2 + \theta_3 g) \\ -\frac{1}{2}k_1(\theta_2 + \theta_3 g) & \frac{1}{2}Mk_1^3 \end{bmatrix} \tag{29}$$

and u_{s2} is required to satisfy the following constrains similar to (18):

$$\begin{array}{ll} \text{i)} & p\{u_{s2} - \varphi_d^T\tilde{\theta} + \tilde{d}\} \le \varepsilon \\ \text{ii)} & pu_{s2} \le 0. \end{array} \tag{30}$$

A specific form of u_{s2} can be obtained using the techniques in Remark 1. For example, similar to (23), this function is chosen as

$$u_{s2} = -\frac{1}{4\varepsilon}h'^2 p \tag{31}$$

where h' is any function satisfying

$$h' \ge ||\theta_M||\,||\varphi_d|| + \delta_d. \tag{32}$$

Remark 3: It is easy to show that $A \ge 0$, if and only if the following condition is satisfied:

$$k_{s1} \ge k_2 + \theta_1 k_1 - \theta_2 - \theta_3 g + \frac{1}{2\theta_1 k_1}(\theta_2 + \theta_3 g)^2. \tag{33}$$

Theorem 2: If the DCARC law (25) is applied, then

A) In general, all signals are bounded. Furthermore, the positive definite function V_s defined by

$$V_s = \tfrac{1}{2}Mp^2 + \tfrac{1}{2}Mk_1^2e^2 \tag{34}$$

is bounded above by

$$V_s \le \exp(-\lambda t)V_s(0) + \frac{\varepsilon}{\lambda}[1 - \exp(-\lambda t)] \tag{35}$$

where $\lambda = \min\{2k_2/\theta_{1\max}, k_1\}$.

B) If after a finite time t_0, there exist parametric uncertainties only (i.e., $\tilde{d} = 0, \forall t \ge t_0$), then, in addition to results in A), zero final tracking error is also achieved, i.e., $e \longrightarrow 0$ and $p \longrightarrow 0$ as $t \longrightarrow \infty$.

Proof: See Appendix II.

Remark 4: The DCARC law (25) has the following advantages: i) since the regressor φ_d depends on the reference trajectory only, the effect of measurement noise is reduced; ii) the regressor φ_d is bounded and can be calculated off-line based on the reference trajectory only to save on-line computation time if needed; iii) due to the use of projection mapping in (10), $\hat{\theta}$ is bounded as shown by P1 of (12). Thus the model compensation u_a in (25) is bounded no matter what type of adaptation law is going to be used. This implies the robust control function u_s may be synthesized totally independent from the design of parameter adaptation law for stability; and iv) gain tuning process becomes simpler since some of the bounds like the first term in the right-hand side of (32) can be estimated off-line. ♢

Remark 5: It is noted that the condition on the selection of robust feedback gain k_{s1} is much less restrictive than those in [14], [13]. This is achieved by judiciously selecting a p.d. function given by (34) instead of the general formulations in [14], [13]. ♢

Remark 6: The motor system is normally equipped with high-resolution position encoder and position measurement feedback is normally quite clean. Comparatively, the velocity measurement is very noisy, which significantly limits the achievable performance. To further alleviate the effect of this noisy velocity feedback, in implementation, the parameter estimates can be updated as follows. Let j represent the sampling instance, ΔT be the sampling period, γ_i be the ith diagonal element of Γ, $\varphi_{d,i}$ be the ith component of φ_d, and $\Theta_i = \hat{\theta}_i(j\Delta T) + \gamma_i \int_{j\Delta T}^{(j+1)\Delta T} \varphi_{d,i} p\, dt$, then the digital implementation of the continuous adaptation law (10) with τ given by (25) is

$$\hat{\theta}_i[(j+1)\Delta T] = \begin{cases} \theta_{i\max}, & \text{if } \Theta_i > \theta_{i\max} \\ \theta_{i\min}, & \text{if } \Theta_i < \theta_{i\min} \\ \Theta_i, & \text{otherwise.} \end{cases} \tag{36}$$

The above digital implementation of parameter estimates needs the feedback of $p = \dot{e} + k_1 e$, which in turn needs the feedback of velocity x_2. Thus, the parameter estimates may be quite noisy if the measurement of the velocity x_2 is noisy. To bypass this problem, one can rewrite Θ_i as

$$\Theta_i = \hat{\theta}_i(j\Delta T) + \gamma_i \int_{j\Delta T}^{(j+1)\Delta T} \varphi_{d,i}(\dot{e} + k_1 e)\, dt. \tag{37}$$

Since $\varphi_d(t)$ depends on the reference trajectory only and its derivative $\dot{\varphi}_d(t)$ can be pre-computed, one can integrate (37) by parts to obtain

$$\Theta_i = \hat{\theta}_i(j\Delta T) + \gamma_i \left(k_1 \int_{j\Delta T}^{(j+1)\Delta T} \varphi_{d,i} e\, dt + \varphi_{d,i} e \Big|_{j\Delta T}^{(j+1)\Delta T} - \int_{j\Delta T}^{(j+1)\Delta T} \dot{\varphi}_{d,i}(t) e\, dt \right). \tag{38}$$

Thus, the parameter estimates implemented through (38) and (36) depend on the desired trajectory and output tracking error only, which are free of velocity measurement noise—another implementation advantage of DCARC. ♢

V. Comparative Experiments

A. Experiment Setup

The experimental set-up shown in Fig. 1 consists of four major components: a precision X–Y stage with two integrated linear drive motors, two linear encoders, a servo controller, and a host PC. The two axes of the X–Y stage are mounted orthogonally on a horizontal plane with Y-axis on top of X-axis. The resolution of the encoders is 1 μm after quadrature. The velocity signal is obtained by the difference of two consecutive position measurements. In the experiments, only Y-axis is used. Standard least-square identification is performed to obtain the parameters of the Y-axis. The

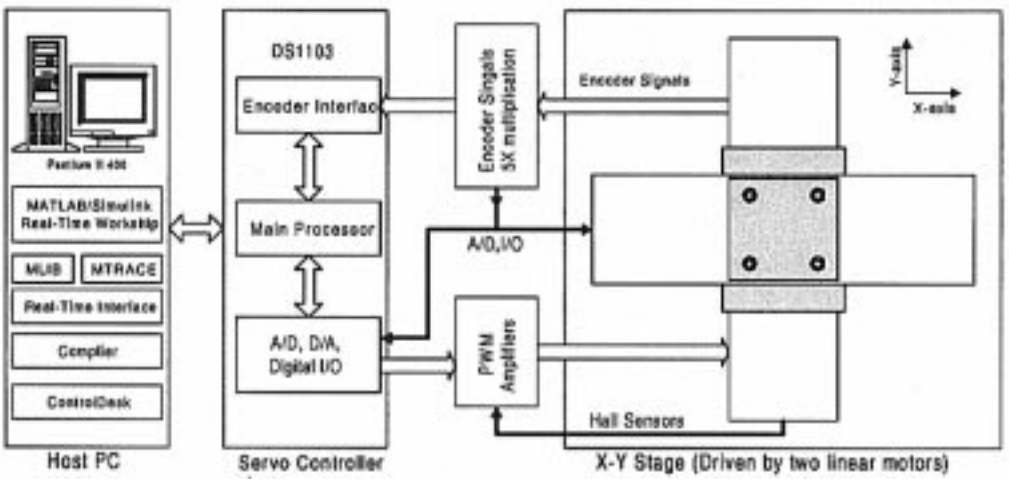

Fig. 1. Experimental setup.

nominal values of M is 0.027 (V/m/s^2). To test the learning capability of the proposed ARC algorithms, we mount a 20-pound load on the motor in experiments and the identified values of the parameters are $\theta_1 = 0.1$ (V/m/s^2), $\theta_2 = 0.273$ (V/m/s), $\theta_3 = 0.09$ (V). The bounds of the parameter variations are chosen as: $\theta_{\min} = [0.02, 0.24, 0.08, -1]^T$ and $\theta_{\max} = [0.12, 0.35, 0.12, 1]^T$.

B. Performance Index

As in [14], [8], the following performance indexes will be used to measure the quality of each control algorithm: I1)

$$L_2[e] = \sqrt{\frac{1}{T_f}\int_0^{T_f} |e|^2\, dt}$$

the scalar valued L_2 norm, is used as an objective numerical measure of *average tracking performance* for an entire error curve $e(t)$, where T_f represents the total running time; I2). $e_M = \max_t\{|e(t)|\}$, the maximal absolute value of the tracking error, is used as an index of measure of *transient performance*; I3). $e_F = \max_{T_f-2\le t\le T_f}\{|e(t)|\}$, the maximal absolute value of the tracking error during the last two seconds, is used as an index of measure of *final tracking accuracy*; I4)

$$L_2[u] = \sqrt{\frac{1}{T_f}\int_0^{T_f} |u|^2\, dt}$$

the average control input, is used to evaluate the amount of *control effort*; I5) $c_u = L_2[\Delta u]/L_2[u]$, the normalized control variations, is used to measure the *degree of control chattering*, where

$$L_2[\Delta u] = \sqrt{\frac{1}{N}\sum_{j=1}^{N} |u(j\Delta T) - u((j-1)\Delta T)|^2}$$

is the average of control input increments.

C. Comparative Experimental Results

Experiments were performed with the Y-axis. The control system is implemented using a dSPACE DS1103 controller board. The controller executes programs at a sampling frequency $f_s = 2.5$ kHz, which results in a velocity measurement resolution of 0.0025 m/s.

The robust control terms u_s in (15) and (25) are implemented as follows. Let k_s be a feedback gain large enough such that

$$k_s \ge k_2 + \frac{1}{4\varepsilon}\, h^2 \tag{39}$$

in which h is defined in (22). Then, $u_s = -k_s p$ satisfies (17) and (18). Similarly, choose a feedback gain k_s' large enough such that

$$k_s' \ge k_{s1} + \frac{1}{4\varepsilon}\, h'^2 \tag{40}$$

where h' is defined in (32). Then, the control function $u_s = -k_s' p$ satisfies (28) and (30). The following four controllers are compared:

PID: PID control with feedforward compensation—the linear motor system described by (5) can be rewritten as

$$\theta_1 \ddot{y}(t) + \theta_2 \dot{y}(t) + \theta_3 S_f(\dot{y}) = u + d. \tag{41}$$

As before, the following variables are available (either measured or computed) for control implementation: $y(t)$, $\dot{y}(t)$, $y_d(t)$, $\dot{y}_d(t)$, and $\ddot{y}_d(t)$. Suppose that the parameters of (14) are known, the control objective can be achieved with the following PID control law with model compensation

$$u = \theta_1 \ddot{y}_d + \theta_2 \dot{y} + \theta_3 S_f(\dot{y}) - K_p e - K_i \int e\, dt - K_d \dot{e}. \tag{42}$$

Closing the loop by applying (42) to (41) easily leads to the closed-loop characteristic equation

$$s^3 + \frac{K_d}{\theta_1}\, s^2 + \frac{K_p}{\theta_1}\, s + \frac{K_i}{\theta_1} = 0. \tag{43}$$

By placing the closed-loop poles at desired locations, the design parameters K_p, K_i and K_d can thus be determined. In the experiments, since the θ_1, θ_2 and θ_3 are unknown parameters, instead of using (42) the following control law is used:

$$u = \hat{\theta}_1(0)\ddot{y}_d + \hat{\theta}_2(0)\dot{y} + \hat{\theta}_3(0) S_f(\dot{y}) \tag{44}$$

$$- K_p e - K_i \int e\, dt - K_d \dot{e} \tag{45}$$

where $\hat{\theta}_1(0)$, $\hat{\theta}_2(0)$, and $\hat{\theta}_3(0)$ are the fixed parameter estimates chosen as 0.05, 0.24, and 0.1, respectively. By placing all the

TABLE I
PERFORMANCE INDEXES FOR SINUSOIDAL TRAJECTORY

controller	set 1 PID	DRC	ARC	DCARC
e_M (μm)	156	56.3	36.1	30.4
e_F (μm)	21.2	11.2	5.1	5.1
$L_2[e]$ (μm)	8.04	5.07	1.99	1.78
$L_2[u]$ (V)	0.20	0.19	0.19	0.19
$L_2[\Delta u]$ (V)	0.06	0.10	0.12	0.09
c_u	0.28	0.56	0.66	0.47

set 2 PID	DRC	ARC	DCARC	set 3 PID	DRC	ARC	DCA
51.2	27.5	26.0	26.0	139	64.2	45.1	43.7
15.1	14.5	6.5	5.5	21.8	12.3	5.2	4.8
2.99	5.81	2.05	1.80	10.1	38.0	3.53	3.17
0.19	0.18	0.19	0.20	0.41	0.41	0.42	0.42
0.05	0.11	0.15	0.09	0.05	0.10	0.12	0.08
0.28	0.64	0.78	0.45	0.13	0.25	0.29	0.19

three closed-loop poles at -300 when $\theta_1 = \theta_{1\min} = 0.02$, one obtains $K_p = 5.4 \times 10^3$, $K_i = 5.4 \times 10^5$, and $K_d = 18$.

ARC: The ARC law proposed in Section III with $u_s = -k_s p$. The continuous function $S_f(x_2)$ is chosen as $(2/\pi)\arctan(900x_2)$. For simplicity, in the experiments, only three parameters, θ_1, θ_3, and θ_4, are adapted. The control gains are chosen as: $k_1 = 400$, $k_s = 32$. The adaptation rates are set as $\Gamma = \mathbf{diag}\{5, 0, 2, 1000\}$. The initial parameter estimates are chosen as: $\hat{\theta}(0) = [0.05, 0.24, 0.1, 0]^T$.

DRC: Deterministic Robust Control—The same control law as the above ARC but without using parameter adaptation, i.e., letting $\Gamma = \mathbf{diag}\{0, 0, 0, 0\}$.

DCARC: The Desired Compensation ARC law proposed in Section IV with $u_s = -k_s' p$. The control gains are chosen as: $k_1 = 400$ and $k_s' = 32$. The adaptation rates are set as $\Gamma = \mathbf{diag}\{25, 0, 5, 1000\}$. For comparison purposes, the same initial conditions as those in ARC are used.

To test the tracking performance of the proposed algorithms, the following two typical reference trajectories are considered.

Case 1—Tracking a Sinusoidal Trajectory $y_r = 0.05\sin(4t)$*:* Comparative experiments are run for tracking a sinusoidal trajectory. The desired trajectory y_d is generated by (24) in which $\beta_1 = 150$, $\beta_2 = 7500$, and $\beta_3 = 125\,000$. The following test sets are performed.

Set 1: To test the tracking performance of the controllers with load, the motor is run with a 20 lb. payload mounted on the motor, which is equivalent to $\theta_1 = 0.1$.

Set 2: To test the performance robustness of the algorithms to parameter variations, the 20 lb. payload is removed, which is equivalent to $\theta_1 = 0.027$.

Set 3: A large step disturbance (a simulated 0.5 V electrical signal) is added around $t = 2.5$ s and removed around $t = 7.5$ s to test the performance robustness of each controller to disturbance.

The experimental results in terms of performance indexes are given in Table I. As seen from the table, in terms of performance indexes e_M and e_F, PID performs poorly for all three sets, but with a slightly lesser degree of control input chattering. One may argue that the performance of PID control can be further improved by increasing the feedback gains. However, in practice, feedback gains have upper limits because the bandwidth of every physical system is finite. To verify this claim, the closed-loop poles of PID controller are placed at -320 instead of -300, which is translated into PID gains of $K_p = 6144$, $K_i = 655\,360$, and $K_d = 19.2$. With these gains, the closed-loop system is found to be unstable in experiments. This indicates that the closed-loop bandwidth that a PID controller can achieve in implementation has been pushed almost to its limit and not much further performance improvement can be expected from PID controllers. Thus, in order to realize the high-acceleration/high-speed/high-accuracy potential of a linear motor system, a PID controller even with feedforward compensation may not be enough.

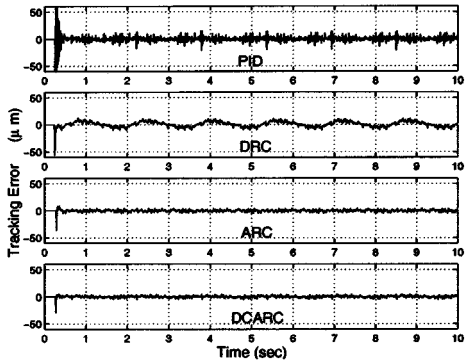

Fig. 2. Tracking errors for sinusoidal trajectory with load.

For Set 1, the tracking errors are given in Fig. 2 (the tracking error of PID control is chopped off). If one compares ARC with DCARC, it is seen that ARC has a relatively poor transient tracking performance. The reason is that only slower adaptation rate Γ can be used for ARC, which reduces the effect of parameter adaptation. When we tried to increase the adaptation rate for ARC further, the system is subjected to quite severe control chattering due to the measurement noises (especially velocity feedback). Comparatively, due to the use of desired compensation structure and the *free-velocity-feedback implementation of parameter adaptation law* presented in Remark 6, DCARC is not so sensitive to velocity measurement noise. In return, a larger adaptation rate can be used for DCARC and the parameter adaptation algorithm of DCARC is able to pick up the actual value of the inertial load more quickly, which can be seen from the parameter estimates shown in Figs. 3 and 4 for ARC and DCARC, respectively. The control inputs of the three controllers are given in Fig. 5. As expected, all controllers use almost the same amount of control effort, and ARC has a larger degree of control input chattering than DCARC.

For Set 2, the tracking errors are given in Fig. 6. It shows that both ARC and DCARC achieve good tracking performance in spite of the change of inertia load. Again, DCARC has the best performance in terms of $L_2[e]$, e_M, and e_F.

The tracking errors for Set 3 are given in Fig. 7. As seen from the figures, the added large disturbance does not affect the performance of ARC and DCARC much, except for the spike when the sudden change of the disturbance occurs. This result illustrates the performance robustness of ARC and DCARC designs. Again, DCARC performs best in terms of $L_2[e]$, e_M, and e_F.

Case 2—High-Acceleration/High-Speed Point-to-Point Motion Trajectory (Without Load): A fast point-to-point desired

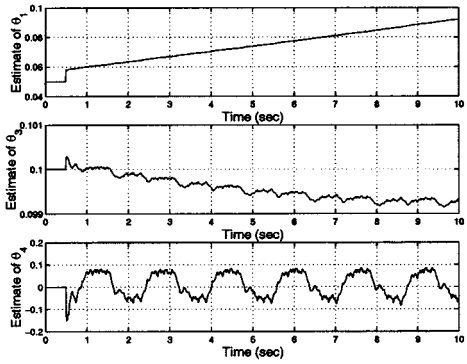

Fig. 3. Parameter estimation of ARC.

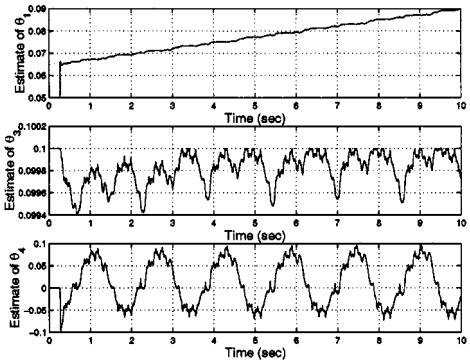

Fig. 4. Parameter estimation of DCARC.

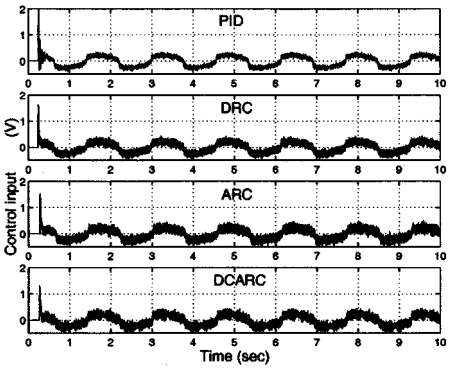

Fig. 5. Control inputs for sinusoidal trajectory with load.

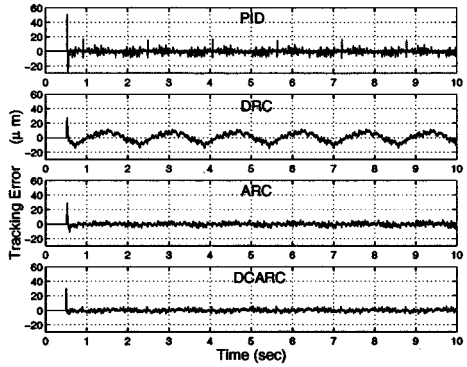

Fig. 6. Tracking errors for sinusoidal trajectory without load.

motion trajectory with high-acceleration/deceleration, which runs back and forth several times, is shown in Fig. 8. The trajectory has a maximum velocity of $v_{\max} = 1$ m/s and a

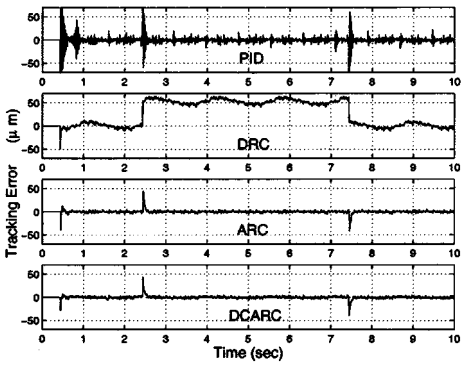

Fig. 7. Tracking errors for sinusoidal trajectory with disturbance.

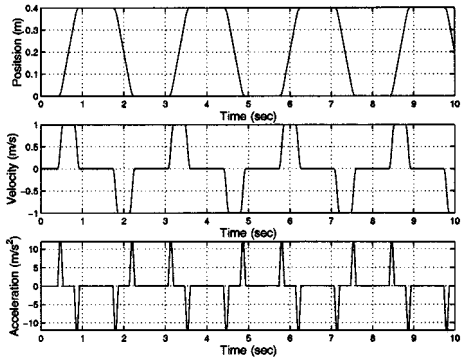

Fig. 8. Point-to-point motion trajectory.

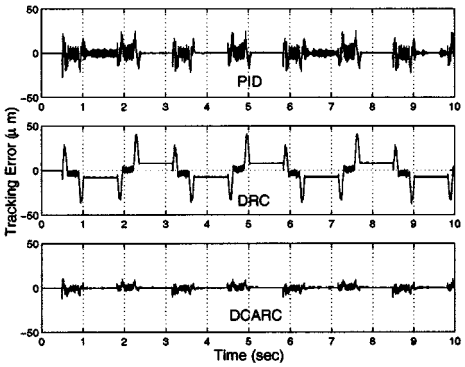

Fig. 9. Tracking errors for point-to-point motion trajectory.

maximum acceleration of $a_{\max} = 12$ m/s^2. The tracking errors of PID, DRC and DCARC are shown in Fig. 9. As seen, the proposed DCARC has a much better performance than PID and DRC. Furthermore, during the zero velocity portion of motion, the tracking error is within ± 1 μm.

Case 3—Nonlinear versus Linear Robust High-Gain Feedback: It is seen from the above experimental results that although ARC and DCARC controllers achieve good tracking performance, tracking errors during transient period or at the moments when the disturbance occurs and disappears, are still relatively large. From the development of ARC and DCARC controllers in Sections III and IV, it can be seen that the smaller ε is and/or the larger the feedback gain k_2 is, the smaller the resulting transient and final tracking error will be [refer to (21) and (35), respectively]. However, this demands a larger lumped robust feedback gain to be used as seen from (39) and (40). In the

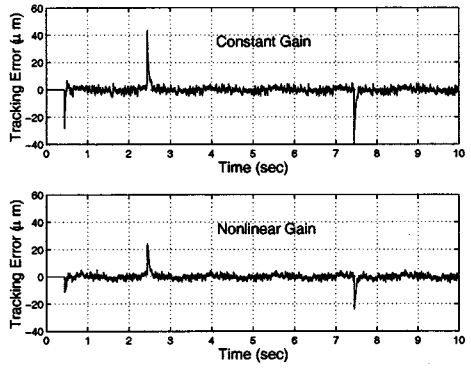

Fig. 10. Tracking errors of DCARC controllers for sinusoidal trajectory with disturbance.

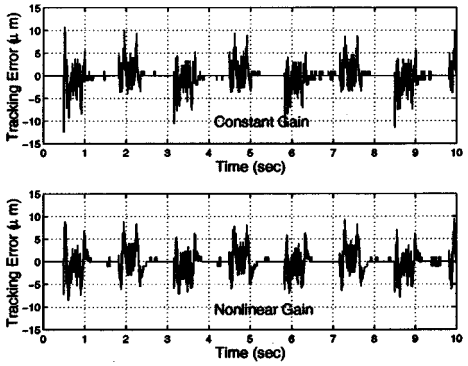

Fig. 11. Tracking errors of DCARC controllers for point-to-point motion.

previous experiments, a constant lumped robust feedback gain (k_s for ARC and k_s' for DCARC) has been used to have a simple implementation. However, such a simplification has the limitation that the lumped robust feedback gain cannot be too large since otherwise the resulting control input may chatter severely due to the amplification of measurement noises. To bypass this implementation problem, in the following, a nonlinear lumped robust feedback gain will be used. Namely, during the nominal tracking period when the tracking error is small, the same level of lumped robust feedback gain as in previous experiments will be used to minimize the effect of measurement noise to keep the control input chattering at a reasonable level. During the transient period when the tracking error is large, a larger lumped robust feedback gain will be used to provide a stronger instantaneous feedback for a better transient tracking performance. Since the proposed ARC strategy is able to use fast adaptation and the transient period is quite short as seen from previous experiments, the increase of control chattering due to the increased feedback gain in the transient may not be noticeable. To illustrate this nonlinear robust feedback gain design concept, in the following, the DCARC controller is used as an example to see the benefit of using such a nonlinear gain.

Choose a nonlinear gain k_s' large enough such that

$$k_s' = \max\left\{k_{p1} + \frac{1}{4\varepsilon'}h'^2,\ k_{p2} + c(|p| - p_0)^2\right\} \geq k_{s1} + \frac{1}{4\varepsilon'}h'^2 \tag{46}$$

where h' is defined in (32), c and p_0 are two empirical parameters. Then, the control function $u_s = -k_s' p$ satisfies (28) and (30). The parameters of the controller are chosen as: $k_1 = 400$, $k_{p1} = 30$, $k_{p2} = 32$, $\varepsilon' = 0.5$, $p_0 = 0.01$, $c = 2 \times 10^6$ whenever $|p| > p_0$ and $c = 0$ whenever $|p| \leq p_0$.

The tracking errors of tracking the sinusoidal trajectory with disturbance are shown in Fig. 10. As expected, the DCARC with a nonlinear robust gain has much smaller transient tracking errors than the constant gain DCARC (i.e., the initial starting period and the periods when the disturbance changes suddenly at $t = 2.5$ s and $t = 7.5$ s). At the same time, the degree of control chattering is kept almost at the same level. The tracking errors of tracking the point-to-point motion trajectory is shown in Fig. 11. Again, the DCARC with the nonlinear robust gain achieves a better tracing performance than the DCARC with a constant feedback gain.

VI. Conclusions

In this paper, an ARC controller and a desired compensation ARC controller have been developed for high performance robust motion control of linear motors with negligible electrical dynamics. The proposed controllers take into account the effect of model uncertainties coming from the inertia load, friction force, force ripple and external disturbances. Theoretically, the resulting controllers guarantee a prescribed transient performance and final tracking accuracy in general while achieving asymptotic tracking in the presence of parametric uncertainties. Furthermore, it is shown that the desired compensation ARC scheme, in which the regressor is calculated using reference trajectory information only, offers several implementation advantages such as less on-line computation time, reduced effect of measurement noise, a separation of robust control design from parameter adaptation, and a faster adaptation rate in implementation. Comparative experimental results are obtained for the motion control of an epoxy core linear motor. Experimental results illustrate the high-performance of the proposed ARC strategies and show the advantages and drawbacks of each method.

Appendix I

Proof of Theorem 1: From (16) and (17), the derivative of V_s is given by

$$\dot{V}_s = -k_2 p^2 + p\{u_{s2} - \varphi^T\tilde{\theta} + \tilde{d}\}. \tag{47}$$

Noting condition i of (18), and choosing $\lambda = \min\{2k_2/\theta_{1\max}\}$, we have

$$\dot{V}_s \leq -k_2 p^2 + \varepsilon \leq -\lambda V_s + \varepsilon \tag{48}$$

which leads to (21) and thus proves the results in A) of Theorem 1. Now consider the situation in B) of Theorem 1, i.e., $\tilde{d} = 0$, $\forall t \geq t_0$. Choose a p.d. function V_a as

$$V_a = V_s + \tfrac{1}{2}\tilde{\theta}^T\Gamma^{-1}\tilde{\theta}. \tag{49}$$

From (47), condition ii of (18) and P2 of (12), the derivative of V_a satisfies

$$\dot{V}_a \leq -k_2 p^2 + \tilde{\theta}^T\Gamma^{-1}\left(\dot{\hat{\theta}} - \Gamma\tau\right) \leq -k_2 p^2. \tag{50}$$

Therefore, $p \in L_2$. It is easy to check that $\dot{p}$ is bounded. So, p is uniformly continuous. By Barbalat's lemma, $p \longrightarrow 0$ as $t \longrightarrow \infty$. □

APPENDIX II

Proof of Theorem 2: Along the trajectory of (26), the time derivative of V_s given by (34) is

$$\dot{V}_s = p\Big\{u_s - \varphi_d^T\tilde{\theta} + (\theta_1 k_1 - \theta_2)\dot{e} \tag{51}$$

$$+\theta_3[S_f(\dot{y}_d) - S_f(x_2)] + \tilde{d}\Big\} + Mk_1^2 e\dot{e}. \tag{52}$$

Applying (27) and (28), and noting $\dot{e} = p - k_1 e$ and $\theta_1 = M$, we have

$$\dot{V}_s \le p\{u_{s2} - \varphi_d^T\tilde{\theta} + \tilde{d}\} + (-k_{s1} + \theta_1 k_1 - \theta_2 - \theta_3 g)p^2 + k_1(\theta_2 + \theta_3 g)ep - Mk_1^3 e^2. \tag{53}$$

If A given by (29) is p.d., then

$$\dot{V}_s \le p\{u_{s2} - \varphi_d^T\tilde{\theta} + \tilde{d}\} - k_2 p^2 - \tfrac{1}{2}Mk_1^3 e^2. \tag{54}$$

With condition i of (30) and $\lambda = \min\{2k_2/\theta_{1\max}, k_1\}$, the derivative of V_s becomes

$$\dot{V}_s \le -\lambda V_s + \varepsilon \tag{55}$$

which leads to (35) and the results in A) of Theorem 2 is proved. Now consider the situation in B) of Theorem 2, i.e., $\tilde{d} = 0$, $\forall t \ge t_0$. Choose a p.d. function V_a as

$$V_a = V_s + \tfrac{1}{2}\tilde{\theta}^T\Gamma^{-1}\tilde{\theta}. \tag{56}$$

From (53), condition ii) of (30), and P2 of (12), the derivative of V_a satisfies

$$\dot{V}_a \le -k_2 p^2 - \tfrac{1}{2}Mk_1^3 e^2 + \tilde{\theta}^T\Gamma^{-1}(\dot{\hat{\theta}} - \Gamma\tau) \le -W \tag{57}$$

where $W = k_2 p^2 + (1/2)Mk_1^3 e^2$. Therefore, $W \in L_1$ and $V_a \in L_\infty$. Since all signals are bounded, it is easy to check that $\dot{W}$ is bounded and thus uniformly continuous. By Barbalat's lemma, $W \longrightarrow 0$ as $t \longrightarrow \infty$, which implies the conclusion of B of Theorem 2. □

REFERENCES

[1] D. M. Alter and T. C. Tsao, "Control of linear motors for machine tool feed drives: Design and implementation of h_∞ optimal feedback control," *ASME J. Dynamic Syst., Meas., Contr.*, vol. 118, pp. 649–656, 1996.

[2] ——, "Dynamic stiffness enhancement of direct linear motor feed drives for machining," in *Proc. American Control Conf.*, 1994, pp. 3303–3307.

[3] P. V. Braembussche, J. Swevers, H. V. Brussel, and P. Vanherck, "Accurate tracking control of linear synchronous motor machine tool axes," *Mechatron.*, vol. 6, no. 5, pp. 507–521, 1996.

[4] S. Komada, M. Ishida, K. Ohnishi, and T. Hori, "Disturbance observer-based motion control of direct drive motors," *IEEE Trans. Energy Conv.*, vol. 6, pp. 553–559, Sept. 1991.

[5] T. Egami and T. Tsuchiya, "Disturbance suppression control with preview action of linear DC brushless motor," *IEEE Trans. Ind. Electron.*, vol. 42, pp. 494–500, Oct. 1995.

[6] G. Otten, T. Vries, J. Amerongen, A. Rankers, and E. Gaal, "Linear motor motion control using a learning feedforward controller," *IEEE/ASME Trans. Mechatron.*, vol. 2, pp. 179–187, Sept. 1997.

[7] K. Ohnishi, M. Shibata, and T. Murakami, "Motion control for advanced mechatronics," *IEEE/ASME Trans. Mechatron.*, vol. 1, pp. 56–67, Mar. 1996.

[8] B. Yao, M. Al-Majed, and M. Tomizuka, "High performance robust motion control of machine tools: An adaptive robust control approach and comparative experiments," *IEEE/ASME Trans. Mechatron.*, vol. 2, pp. 63–76, June 1997.

[9] B. Yao and L. Xu, "Adaptive robust control of linear motors for precision manufacturing," in *Proc. 14th IFAC World Congr.*, Vol. A, Beijing, China, 1999, pp. 25–30.

[10] B. Yao and M. Tomizuka, "Smooth robust adaptive sliding mode control of robot manipulators with guaranteed transient performance," *Trans. ASME, J. Dyn. Syst., Meas. Contr.*, vol. 118, no. 4, pp. 764–775, 1996.

[11] ——, "Adaptive robust control of SISO nonlinear systems in a semi-strict feedback form," *Automatica*, vol. 33, no. 5, pp. 893–900, 1997.

[12] B. Yao, "High performance adaptive robust control of nonlinear systems: A general framework and new schemes," in *Proc. IEEE Conf. Decision and Control*, 1997, pp. 2489–2494.

[13] ——, "Desired compensation adaptive robust control," in *Proc. ASME Dynamic Systems and Control Division, IMECE'98*, vol. DSC-64, 1998, pp. 569–575.

[14] B. Yao and M. Tomizuka, "Comparative experiments of robust and adaptive control with new robust adaptive controllers for robot manipulators," in *Proc. IEEE Conf. Decision and Control*, 1994, pp. 1290–1295.

[15] C. C. de Wit, H. Olsson, K. J. Astrom, and P. Lischinsky, "A new model for control of systems with friction," *IEEE Trans. Automat. Contr.*, vol. 40, no. 3, pp. 419–425, 1995.

[16] A. Brian and D. Pierre, "A survey of models, analysis tools and compensation methods for the control of machines with friction," *Automatica*, vol. 30, no. 7, pp. 1083–1138, 1994.

[17] S. Sastry and M. Bodson, *Adaptive Control: Stability, Convergence and Robustness*. Englewood Cliffs, NJ: Prentice-Hall, 1989.

[18] G. C. Goodwin and D. Q. Mayne, "A parameter estimation perspective of continuous time model reference adaptive control," *Automatica*, vol. 23, no. 1, pp. 57–70, 1989.

[19] M. Krstic, I. Kanellakopoulos, and P. V. Kokotovic, *Nonlinear and Adaptive Control Design*. New York: Wiley, 1995.

[20] N. Sadegh and R. Horowitz, "Stability and robustness analysis of a class of adaptive controllers for robot manipulators," *Int. J. Robot. Res.*, vol. 9, no. 3, pp. 74–92, 1990.

Li Xu received the B.S. degree from the University of Electronic Science and Technology of China, Chengdu, China, and the M.S. degree from Tsinghua University, Beijing, China, in 1991 and 1997, respectively. He is currently pursuing the Ph.D. degree at the School of Mechanical Engineering at Purdue University, West Lafayette, IN.

His research interests include coordinated control of electro-mechanical systems, adaptive robust control, and nonlinear observer design.

Mr. Xu was the recipient of the Best Student Paper Award at the *2000 IEEE Conference on Control Applications (CCA)*, and a finalist for the ASME Dynamic System and Control Division Student Best Paper Award at the 2000 International Mechanical Engineering Congress and Exposition (IMECE).

Bin Yao (S'92–M'96) received the Ph.D. degree in mechanical engineering from the University of California at Berkeley, Berkeley, in 1996.

Since 1996, he has been an Assistant Professor in the School of Mechanical Engineering at Purdue University, West Lafayette, IN. His research interests include design and coordinated control of intelligent high performance electro-mechanical/electro-hydraulic systems, optimal adaptive and robust control, nonlinear observer design and neural networks for virtual sensing, modeling, fault detection, diagnostics, and adaptive fault-tolerant control, and data fusion.

Dr. Yao is the recipient of the 1997 Caterpillar Engineering Young Faculty Development Fund for his work on the electro-hydraulic control, and the 1998 National Science Foundation CAREER Award for his work on the engineering synthesis of high performance adaptive robust controllers for mechanical systems and manufacturing processes.